
Molecular Biologic and Scintigraphic Analyses of Somatostatin Receptor-Negative Meningiomas

Christian Meewes, Karl H. Bohuslavizki, Brigitte Krisch, Janka Held-Feindt, Eberhard Henze, and Malte Clausen

Department of Dermatology, University of Cologne, Cologne; Department of Nuclear Medicine, University Hospital Eppendorf, Hamburg; and Department of Anatomy and Clinic of Nuclear Medicine, Christian-Albrechts-University, Kiel, Germany

Somatostatin receptor scintigraphy (SRS) using ^{111}In -octreotide has proven useful in the preoperative discrimination of expansive central nervous system lesions. Meningiomas, generally expressing human somatostatin receptor (hsst) on their surface, were detected with a sensitivity of about 100%. This finding was associated with the assumption that meningiomas lack an intact blood-brain barrier. However, this exclusion procedure became questionable when histologically proven meningiomas in which SRS was negative were reported. Therefore, the aim of this study was to discover why these meningiomas gave negative SRS results. **Methods:** Before surgery, 46 patients with 47 meningiomas underwent standard MRI and SRS. Thirty-four of these patients with 35 tumors were also examined by $^{99\text{m}}\text{Tc}$ -diethylenetriaminepentaacetic acid (DTPA) brain scintigraphy. After surgical resection, hsst subtype 2 (hsst2) messenger RNA (mRNA) expression of 4 SRS-positive and 4 SRS-negative meningiomas was estimated semiquantitatively by reverse transcriptase polymerase chain reaction (RT-PCR). Translation of hsst2 mRNA into receptor proteins was proven immunocytochemically on the surface of 1 SRS-positive and 1 SRS-negative meningioma. Tumor specimens used for RNA extraction and RT-PCR and cultivated cells used for hsst2 immunostaining were tested for their meningioma nature by immunocytochemistry. **Results:** SRS yielded positive results in 39 meningiomas with a tumor volume of 24.1 ± 32.8 mL and negative results in 8 meningiomas with a volume of 3.9 ± 6.5 mL. $^{99\text{m}}\text{Tc}$ -DTPA scintigraphy visualized 24 of 35 meningiomas. SRS was positive in all of them. In contrast, 11 meningiomas were $^{99\text{m}}\text{Tc}$ -DTPA negative. In these meningiomas, SRS was negative in 5 cases (5.4 ± 8.1 mL), whereas the remaining 6 were positive (4.6 ± 4.5 mL). None of the meningiomas was $^{99\text{m}}\text{Tc}$ -DTPA positive and SRS negative. RT-PCR revealed no significant difference of hsst2 mRNA expression between SRS-positive and SRS-negative meningiomas but showed varied expression among all meningiomas regardless of SRS results. Furthermore, hsst2 proteins were visualized immunocytochemically on the surface of cultivated cells of SRS-positive and SRS-negative meningiomas. **Conclusion:** SRS-negative meningiomas do express hsst2; thus, in these meningiomas SRS is false-negative. Because an insufficient sensitivity was excluded, $^{99\text{m}}\text{Tc}$ -DTPA scintigraphy identified a permeability barrier in SRS-negative meningiomas that explains their false-negative SRS results. SRS-negative meningiomas most likely meet the function of

their tissue of origin (the meninges) to develop more-or-less intact permeability barriers.

Key Words: human somatostatin receptor; somatostatin receptor scintigraphy; $^{99\text{m}}\text{Tc}$ -DTPA brain scintigraphy; reverse transcriptase polymerase chain reaction; immunohistochemistry; immunocytochemistry; meningioma; leptomeninges; blood-brain barrier; blood-tumor barrier

J Nucl Med 2001; 42:1338-1345

The cyclic tetradecapeptide somatostatin (SRIF-14), originally isolated as a hypothalamic somatotropin release-inhibiting factor, is widely distributed throughout the central nervous system and peripheral tissues (1). Its various effects (2-5) are mediated by 5 different transmembranous somatostatin receptor subtypes (sst1-sst5), which show distinct tissue distributions and differ in their affinity to the extended form of the somatostatin peptide (SRIF-28) and to synthetic derivatives. Somatostatin receptors have been identified on the surface of numerous cell types in vitro by different methods (4,6) and in vivo by means of somatostatin receptor scintigraphy (SRS) using ^{111}In -octreotide (7). Application of SRS to successfully allow visualization and localization of sst-expressing tumors, including gastroenteropancreatic tumors (8), malignant lymphoma (9), small cell lung cancer (10,11), and meningiomas, has been reported (12-15). SRS studies have shown repeatedly in vitro and in vivo that meningiomas, regardless of their histologic grading, express human sst (hsst) with a sensitivity of approximately 100% (12-15). The extremely high sensitivity of about 100% of meningiomas in SRS was, among other things, associated with the assumption that meningiomas lack an intact blood-brain barrier (13-17). Because the somatostatin analog ^{111}In -octreotide, used as a tracer in SRS, is a polar, water-soluble octapeptide, it may penetrate only into those tumors that do not develop, or have a disrupted, blood-brain barrier (18,19). Therefore, SRS has been suggested for the preoperative differentiation of meningiomas from neurinomas, which show a predilection for similar sites and do not express hsst (16). If no tracer accumulation was detectable, meningiomas were supposed to be excluded. However, this procedure became questionable with reports of histologically proven meningiomas in

Received Dec. 29, 2000; revision accepted May 14, 2001.

For correspondence or reprints contact: Karl H. Bohuslavizki, MD, PhD, Department of Nuclear Medicine, University Hospital Eppendorf, Martini-strasse 52, D-20246 Hamburg, Germany.

which SRS was found to be negative (12,20). Neither histology nor localization of the meningiomas correlated with the lack of tracer uptake. In contrast, a small tumor volume was associated with a negative SRS result. Because technical reasons, such as radiopharmacy or image acquisition factors, could clearly be excluded, the reasons for negative SRS results of meningiomas remained unclear. Besides the possibility that SRS-negative meningiomas indeed do not express hst2 on their cell surface—and therefore the result would be true-negative—several particularities of these meningiomas could lead to a false-negative SRS result in the case of a positive *in vitro* receptor finding (21). Therefore, the purpose of this study was to discover why these meningiomas had negative SRS results.

MATERIALS AND METHODS

Between February 1996 and October 1997, 46 adult patients (34 women, 12 men; mean age, 59.1 ± 13.2 y; age range, 20–87 y) with 47 meningiomas were referred for SRS before neurosurgical treatment. Meningiomas were either proven or suspected on the basis of MRI in these patients. In addition to SRS, brain scintigraphy using ^{99m}Tc -diethyleneaminepentaacetic acid (DTPA) as a nonspecific tracer for a permeability barrier (e.g., blood–brain barrier integrity) was performed on 34 patients with 35 tumors.

Surgical specimens were fixed in 4% formaldehyde and embedded in paraffin for histopathologic examination. Sections (4- μm thick) were stained with hematoxylin–eosin and with elastica van Gieson.

MRI was performed on either a 1.5-T Magnetom Vision (Siemens, Erlangen, Germany) or a 1.0-T Magnetom Expert (Siemens) scanner. T1-weighted (repetition time [TR], 500 ms; echo time [TE], 12 ms) and T2-weighted spin-echo sequences (TR, 3,600 ms; TE, 98 ms) were acquired with a slice thickness of 6–8 mm. Gadolinium-DTPA (Schering, Berlin, Germany) was administered intravenously at a dosage of 0.1 mmol/kg body weight for contrast enhancement. Tumor volumes were calculated from MR images under the assumption of a rotational ellipsoid.

After intravenous injection of 100–200 MBq ^{111}In -octreotide (Mallinckrodt, Petten, The Netherlands), digital whole-body acquisitions were obtained simultaneously in anterior and posterior projection at 10 min and at 1, 4, and 24 h with a scan speed of 10 cm/min. A large-field-of-view gamma camera equipped with a medium-energy, parallel-hole collimator (Bodyscan; Siemens, Erlangen, Germany) was used. The energy window was adjusted to both ^{111}In peaks at 173 and 247 keV, each with a symmetric 20% window.

In addition, SPECT was performed at 4 and 24 h with a single-head, large-field-of-view gamma camera equipped with a medium-energy, parallel-hole collimator (Diacam; Siemens). The 360° data were acquired for 64 angles in a step-and-shoot mode, and projections were stored in a 128 × 128 matrix. SPECT data were reconstructed by filtered backprojection using a Butterworth filter of fifth order and a cutoff frequency of 0.23 of the Nyquist frequency.

Evaluation of the scintigrams was performed independently by 2 nuclear medicine physicians. Results were considered negative if neither identified tracer accumulations on any of the scintigrams; otherwise, results were positive.

One hour after intravenous injection of 600 MBq ^{99m}Tc -DTPA, SPECT was performed with a triple-head, large-field-of-view gamma camera equipped with low-energy, high-resolution collimators (Multispect 3; Siemens). The 360° data were acquired for 72 angles in a step-and-shoot mode, and projections were stored in a 128 × 128 matrix. SPECT data were again reconstructed by filtered backprojection using a Butterworth filter of fifth order and a cutoff-frequency of 0.3 of the Nyquist frequency. Evaluation was performed as described for SRS.

After surgical resection, sterile samples of the meningioma were macroscopically liberated from vessels and subsequently dissociated in 0.075% trypsin for 30 min at 37°C. Thereafter, cells were resuspended in Dulbecco's modified Eagle's medium containing 5% horse serum, 5% fetal calf serum, 100 $\mu\text{g}/\text{mL}$ penicillin/streptomycin, and 2.5 $\mu\text{g}/\text{mL}$ amphotericin B. Aliquots of 4–5 × 10⁶ cells were placed in 75-cm² tissue culture flasks and cultivated at 37°C in 5% CO₂/95% air with 100% humidity. For immunocytochemical experiments, monolayer cultures were prepared by placing 100,000 cells on sterile poly-D-lysine-coated coverslips.

RNA was isolated from samples of 4 SRS (^{111}In -octreotide)-positive (OP1–OP4) and 4 SRS (^{111}In -octreotide)-negative (ON1–ON4) meningiomas by using a Qiagen total RNA kit (Qiagen, Hilden, Germany). Before reverse transcription, 500 ng RNA were subjected to a deoxyribonuclease (DNase) I digestion by adding 1 μL of 10× DNase incubation buffer (GIBCO-BRL, Eggenstein, Germany) and 10 U ribonuclease (RNase)-free DNase I (Boehringer, Mannheim, Germany) in a final volume of 10 μL for 20 min at 25°C to destroy genomic DNA. DNase was then inactivated by incubation with 1 μL 20 mmol/L ethylenediaminetetraacetic acid (EDTA) for 15 min at 65°C. The reverse transcription mixture containing 2 μL 10× polymerase chain reaction (PCR) buffer IV (Biomol, Hamburg, Germany), 2 μL 10 mmol/L desoxynucleoside triphosphates, 2 μL 100 mmol/L dithiothreitol, 2 μL 25 mmol/L MgCl₂, and 1 μL (100 ng/ μL) oligo(dT)₁₅ primer (Boehringer) was added to a final volume of 20 μL . After incubation for 5 min at 65°C and 5 min at 0°C, reverse transcription was performed after adding 100 U superscript RNase H⁻ reverse transcriptase (RT) (GIBCO-BRL) for 75 min at 37°C and stopped by incubation for 5 min at 95°C. Each probe was divided into 2 equal volumes and used for amplification of hst2 and human β -actin (h β -actin)-specific complementary DNA. For amplification, PCR mixture containing 4 μL 10× PCR buffer IV, 0.5 μL (10 pmol/ μL) each of PCR sense/antisense primers of hst2 or h β -actin, and 4 μL (hst2) or 2 μL (h β -actin) 25 mmol/L MgCl₂ was added to a final volume of 50 μL . After initial denaturation at 94°C for 1 min, the following cycling conditions were started with 2.5 U Taq DNA polymerase (Biomol): initial denaturation at 94°C for 5 min, 94°C for 1 min, 54°C for 1 min, and 72°C for 1.5 min. The 40-cycle thermal profile included a final 10-min and 72°C extension step. Aliquots of 12 μL each of the amplification mixtures were examined by 2% agarose gel electrophoresis in 90 mmol/L Tris, 90 mmol/L boric acid, and 20 mmol/L EDTA. Control reactions were performed by omitting RNA. Primers for hst2 were 5'-CGG-AGC-AAC-CAG-TGG-GGG-A-3' and 5'-GG-GTT-GGC-ACA-GCT-GTT-AGC-3'; fragment, 377 base pairs (bp). Primers for h β -actin were 5'-ACG-CCT-CTG-GCC-GTA-CCA-CTG-GCA-TCG-3' and 5'-CTT-GCT-GAT-CCA-CAT-CTG-CTG-GAA-GGT-G-3'; fragment, 650 bp.

Immunochemical experiments were performed to confirm the meningioma nature of the tumor resection samples used for RNA isolation and RT-PCR and of the cell cultures used for visualiza-

tion of human somatostatin receptor subtype 2 (hsst2). An antibody against the astroglial marker glial fibrillary acid protein (GFAP) (22) was used to exclude possible contamination with hsst-expressing glial cells. Meningioma cells were identified using an antibody against the glycoprotein fibronectin, which is expressed by fibroblasts and cells of meningeal origin but not by glial cells. In addition, cell cultures were tested for their immunoreactivity for von Willebrand's factor (vWF) and CD-68 to exclude contaminating endothelial cells and macrophages.

For immunohistochemical examination, two 4- μ m sections of ON4 and OP4 were mounted on adhesion slides (Shandon, Frankfurt, Germany) and dried overnight at 37°C. Sections were dewaxed in HistoClear (Shandon) and rehydrated. The sections used for fibronectin immunostaining were heated 15 min in 10 mmol/L citrate buffer, pH 6.0. After blocking endogenous peroxidase activity with 3% hydrogen peroxide for 10 min, sections were rinsed in Tris buffer (50 mmol/L Tris[hydroxymethyl]aminomethane containing 38 μ L/mL 1N chloric acid, pH 7.6). Nonspecific binding was blocked by incubation for 20 min at room temperature with normal swine serum (for fibronectin staining; Dako, Glostrup, Denmark) or normal rabbit serum (for GFAP staining; Dako), each diluted 1:20 in Tris buffer. Sections were incubated for 1 h at 37°C with polyclonal rabbit antihuman fibronectin antibody (diluted 1:200 with Tris buffer containing 1% bovine serum albumin; Dako) and with monoclonal mouse antihuman GFAP antibody (diluted 1:1,000 with Tris buffer containing 1% bovine serum albumin; Dako). Sections were then washed 3 times for 5 min in Tris buffer. Thereafter, the biotinylated secondary swine antirabbit and rabbit antimouse antibodies (each diluted 1:200 with Tris buffer; Dako) were applied for 30 min at 37°C. Sections were washed again in Tris buffer before and after incubation for 20 min at 37°C with peroxidase-conjugated streptavidin (diluted 1:300 with Tris buffer; Dako). Bound peroxidase was visualized by the reaction with the chromogen 3-amino-9-ethylcarbazole (Sigma, St. Louis, MO) containing 0.015% hydrogen peroxide, and cells were counterstained with Mayer's hemalum (diluted 1:5; Merck, Darmstadt, Germany) and viewed by light microscopy (Axiophot; Zeiss, Oberkochen, Germany).

For immunocytochemical identification of cultivated meningioma cells, an avidin-biotin complex peroxidase method-based kit (Universal Immunostaining kit; Coulter Immunotech, Marseille, France) was used. Monolayers of meningioma cells were washed twice at 37°C in phosphate-buffered saline (PBS; Seromed, Berlin, Germany) before and after fixation in ice-cold acetone (Merck) for 10 min. After incubation with protein blocking agent for 10 min, 1:100 dilutions of monoclonal mouse antihuman GFAP, polyclonal rabbit antihuman fibronectin, monoclonal mouse antihuman vWF (all Dako), and monoclonal antihuman CD-68 antibodies (23) were applied. After overnight incubation at 4°C, all of the following steps were performed. Finally, cells were counterstained with Mayer's hemalum and viewed by light microscopy.

Somatostatin receptor subtype 2 protein on the surface of cultivated cells of the OP4 and ON4 meningioma was detected by immunocytochemistry. Polyclonal primary antibodies were generated in 2 rabbits against the amino acids 43–53 (QTEPYDLTSN) of the human somatostatin receptor subtype 2 protein. The antibody was purified from rabbit serum by affinity chromatography. Although the antigenic sequences of previously published hsst2 antibodies (24) were located intracellularly, and, therefore, cells had to be fixed and permeabilized before immunostaining, the

target sequence of this antibody is located extracellularly, directly neighboring the cell surface; thus, it does not participate in the ligand binding. Therefore, fixation or permeabilization of the cells that might lead to a loss of antigen reactivity is not needed but the antibody can be used for hsst2 immunostaining on the surface of living, intact cells. Monolayers of meningioma cells grown on coverslips were washed with Gey's buffered salt solution (GIBCO-BRL, Eggenstein, Germany) supplemented with 0.6% glucose and 6 mmol/L MgCl₂, cooled down stepwise to 4°C, incubated with a 1:100 dilution of the polyclonal rabbit anti-hsst2 antibody for 2.5 h at 4°C, and washed again in the same buffer. Control reactions were performed by preincubating the primary antibody with a surplus of its antigenic peptid (haptene) for 30 min at 37°C. Cells were then fixed in 3% glutardialdehyde for 30 min at room temperature, subsequently washed in PBS, and incubated for 15–20 min in 0.1 mol/L lysine (Merck) in PBS. Coverslips were again washed twice in PBS. Coverslips were then incubated overnight at 4°C with a 1:30 dilution of the gold-labeled secondary polyclonal goat antirabbit antibody (GAR-GP-ULTRA SMALL; Aurion, Wageningen, The Netherlands) in PBS containing 0.2% of gelatin (Aurion, Cologne, Germany). Thereafter, coverslips were washed extensively in PBS containing 0.1% gelatin, twice in PBS, once in 10 mmol/L EDTA, and twice in doubly distilled water before cells were incubated with silver enhancer (Aurion R-Gent; Aurion, Cologne, Germany) for 20–35 min at room temperature. Finally, coverslips were washed 4 times in doubly distilled water for 5 min each, counterstained with Mayer's hemalum, and viewed by light microscopy.

RESULTS

MRI revealed pronounced and homogenous contrast enhancement in T1-weighted spin-echo sequences in all 47 meningiomas of the 46 patients. Figure 1 shows examples of coronal images of OP4 and ON4 meningiomas.

Visual analyses exhibited positive somatostatin receptor scintigrams in 39 meningiomas with a mean tumor volume of 24.1 ± 32.8 mL (sic) (Figs. 2A and 2B). In contrast, no tracer accumulation was observed in any of the obtained somatostatin receptor scintigrams of 8 histologically proven meningiomas (Figs. 3A and 3B). The volume of these ON meningiomas amounted to 3.9 ± 6.5 mL (sic) and was significantly lower than the volume of OP meningiomas. Neither a correlation with the localization or with histologic types of the meningiomas was observed. OP meningiomas were distributed among 14 different localizations and ON meningioma among 5 different localizations. Histologically, OP meningiomas were meningotheliomatous ($n = 22$), fibroblastic ($n = 7$), transitional cellular ($n = 6$), psammomatous ($n = 1$), atypical ($n = 2$), or malignant ($n = 1$), whereas ON meningiomas were meningotheliomatous ($n = 5$), fibroblastic ($n = 2$), or psammomatous ($n = 1$).

^{99m}Tc-DTPA scintigraphy visualized 24 of 35 examined meningiomas as shown in Figure 2C (volume, 28.2 ± 33.9 mL [sic]). All of them showed an even stronger accumulation of ¹¹¹In-octreotide in SRS. In contrast, 11 meningiomas remained undetected by ^{99m}Tc-DTPA scintigraphy as shown in Figure 3C. Of these, SRS was negative in 5 cases (volume, 5.4 ± 8.1 mL), whereas the remaining 6 meningiomas

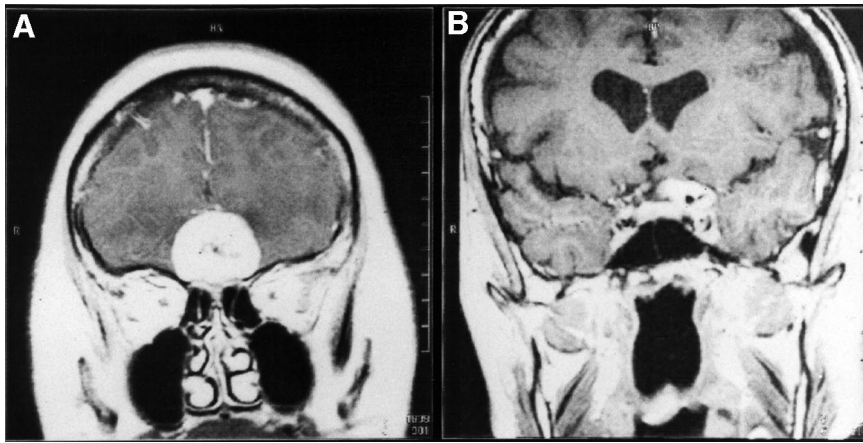


FIGURE 1. Coronal gadolinium-DTPA-enhanced T1-weighted MRI slices of SRS OP4 meningioma (A) and SRS ON4 meningioma (B).

were SRS positive (volume, 4.6 ± 4.5 mL). Interestingly, no meningioma was positive for ^{99m}Tc -DTPA but negative for ^{111}In -octreotide. Table 1 summarizes the results of ^{99m}Tc -DTPA scintigraphy with respect to the SRS result and the tumor volume.

Somatostatin receptor subtype 2–specific messenger RNA (mRNA) expression of 4 OP and 4 ON meningiomas was estimated by RT-PCR. Although this is not a quantitative method, the occurrence of amplicates after a certain numbers of cycles with the same amount of mRNA and the simultaneous amplification of a high-copy transcript such as $\text{h}\beta$ -actin out of the same complementary DNA as reference yields semiquantitative results when comparing different samples. Before the isolation of RNA that was used for RT-PCR, immunohistochemical experiments were performed to confirm the meningioma nature of the tumor samples. None of the meningiomas exhibited immunoreactivity for the astroglial marker GFAP. Therefore, contamination with hsst2 -expressing glial cells that could have led

to false-positive RT-PCR results was excluded. In contrast, almost all cells were strongly immunoreactive for fibronectin, which further confirms the histologic diagnosis. As shown in Figure 4, all examined OP and ON meningiomas expressed hsst2 and $\text{h}\beta$ -actin mRNA, though in different amounts. For example, OP4, ON1, ON2, and ON4 meningiomas exhibited almost the same signal intensity for $\text{h}\beta$ -actin, whereas the corresponding hsst2 signals were stronger in ON1 and ON2 than in OP4 and ON4 meningiomas; this finding indicates a higher expression of hsst2 in ON1 and ON2 than in OP4 and ON4 meningiomas. Taken together, RT-PCR revealed no significant difference of hsst2 mRNA expression between OP and ON meningiomas but showed varied hsst2 expression among all meningiomas, regardless of SRS results.

In addition to analyses of hsst2 mRNA, the receptor protein was visualized on the surface of cultivated cells of OP4 and ON4 meningiomas using an antibody specifically directed against amino acids 43–53 of the hsst2 protein and

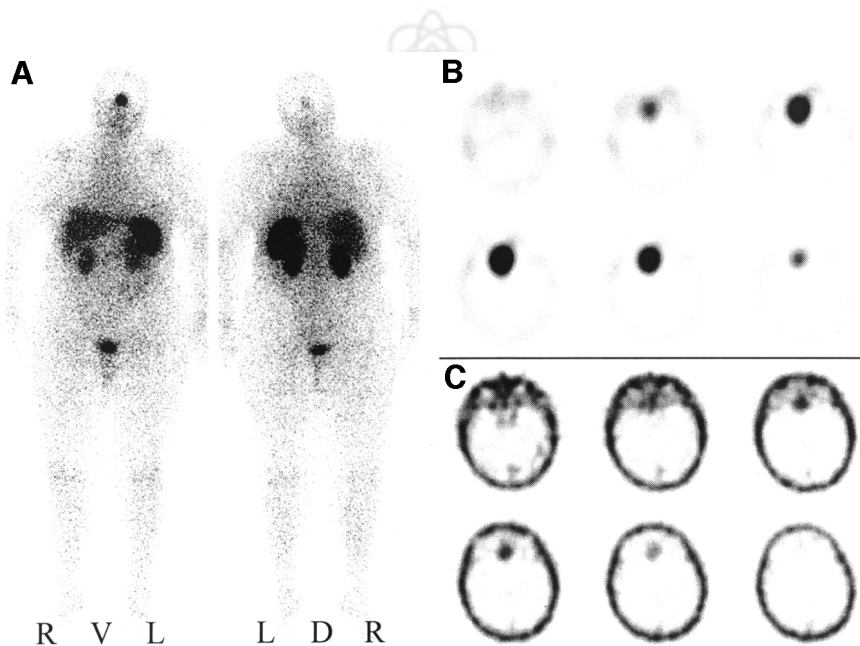


FIGURE 2. SRS and ^{99m}Tc -DTPA scintigraphy of SRS OP4 meningioma. (A) Planar somatostatin receptor scintigram 4 h after injection of 200 MBq ^{111}In -octreotide in anterior and posterior projection. R = right; L = left; V = ventral; D = dorsal. (B) Corresponding transverse SPECT slice at 4 h. (C) Transverse SPECT slice 1 h after injection of 600 MBq ^{99m}Tc -DTPA.

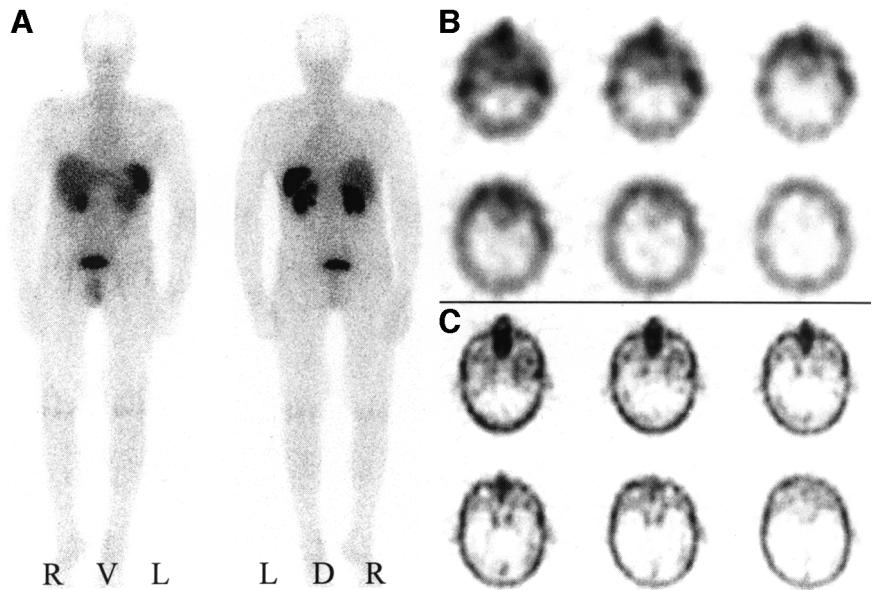


FIGURE 3. SRS and ^{99m}Tc -DTPA scintigraphy of SRS ON4 meningioma. (A) Planar somatostatin receptor scintigram 4 h after injection of 200 MBq ^{111}In -octreotide in anterior and posterior projection. R = right; L = left; V = ventral; D = dorsal. (B) Corresponding transverse SPECT slice at 4 h. (C) Transverse SPECT slice 1 h after injection of 600 MBq ^{99m}Tc -DTPA.

its localization through a gold-labeled secondary antibody followed by silver intensification. In accordance with immunohistochemistry, the nature of cultivated meningioma cells was verified to avoid false-positive results. Almost all OP4 and ON4 cells exhibited strong immunoreactivity for fibronectin, but none of them showed positive staining for GFAP. In addition, <1% of cells was positive for anti-vWF and anti-CD-68, respectively, which indicates that the number of contaminating endothelial cells and macrophages was comparatively low. In OP4 and ON4 meningiomas, immunoreactivity for *hsst2* was detected at the light-microscopic level as shown in Figures 5A and 5B. Preincubation of the primary antibody with a surplus of its antigenic peptide abolished receptor staining as shown in Figures 5C and 5D. Both meningiomas showed the same distribution of immunostained somatostatin receptor subtype 2 proteins on their surface: The silver particles, indicating bound anti-*hsst2* antibodies, decorated the processes and somata of numerous (but not all) cells in a fine, stippled pattern (Figs. 5A and 5B). However, a difference in the density of immunostained *hsst2* was noticed between the 2 meningiomas. Although most ON4 cells were intensively stained and *hsst2* proteins appeared to be densely packed, the density of *hsst2* proteins on the surface of OP4 cells seemed to be markedly lower (Figs. 5A and 5B).

TABLE 1

Results of ^{99m}Tc -DTPA Scintigraphy, SRS, and Respective Number (*n*) and Tumor Volume

Group	DTPA	SRS	<i>n</i>	Volume (mL)
1	Positive	Positive	24	28.2 ± 33.9
2	Negative	Positive	6	4.6 ± 4.5
3	Negative	Negative	5	5.4 ± 8.1

DISCUSSION

Because meningiomas and neurinomas show a predilection for similar sites (e.g., cerebellopontine angle, cavernous sinus, or spine), but surgical treatment may require different strategies because of different biologic behavior, preoperative discrimination is desired by the neurosurgeon. In addition to MRI, which allows successful discrimination of meningiomas and neurinomas in most cases (25), SRS was suggested for further differentiation on a functional basis. *In vivo* and *in vitro* studies have shown repeatedly that meningiomas express *hsst* (12–15), whereas neurinomas are completely devoid of *hsst* (16). This exclusion procedure became questionable when we reported histologically proven meningiomas in which SRS was negative (12,20). In contrast to localization and histologic type of meningioma, a small tumor volume was associated with a negative SRS result. Because technical reasons were excluded and the underlying reason remained unclear, the purpose of this study was to discover why negative SRS meningioma results occurred.

To investigate whether the observed negative SRS results were true-negative or false-negative, *hsst* expression of SRS OP and SRS ON meningiomas was compared, on both mRNA and the protein level. Because the 8-amino acid somatostatin analog octreotide interacts with only 3 of 5 known somatostatin receptor subtypes (*hsst1*–*hsst5*), with the highest affinity to *hsst2* and a much lower affinity to *hsst3* and *hsst5* (26,27), meningiomas were tested for their expression of *hsst2*. Semiquantitative estimation of *hsst2* mRNA expression by RT-PCR revealed no significant difference between OP and ON meningiomas but showed varied *hsst2* expression among all meningiomas, regardless of SRS results. Various authors have reported that the mRNA level of *hsst1*–*hsst5* was accompanied with a cor-

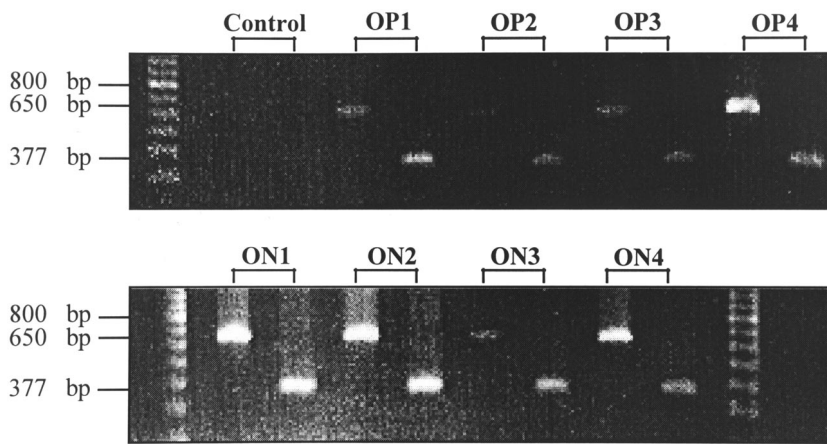


FIGURE 4. Ethidium bromide-stained agarose electrophoresis gel after separating RT-PCR amplificates with primers of *hsst2* (377 bp) and *hβ-actin* (650 bp) from 4 SRS OP1–OP4 meningiomas (top) and 4 SRS ON1–ON4 meningiomas (bottom). Control reactions were performed by omitting RNA. Sizes (bp) of marker fragments are indicated (left lane, top; left and right lanes, bottom).

responding level of its protein (27–29). *hsst3* was expressed on mRNA only in the cerebellum and not on the protein level (28). To prove that *hsst2* mRNA is translated into the receptor protein on the cell surface of ON meningiomas, immunocytochemical visualization was performed. We found *hsst2* expression on the surface of cultivated cells of OP and ON meningiomas, with a higher density on ON meningioma cells. Culture conditions possibly led to a selection of cells that exhibited stronger *hsst2* expression than did the average tumor cell of the ON meningioma because no difference of *hsst2* expression was observed on the mRNA level. However, our *in vitro* studies clearly indicated that the results of SRS-negative meningiomas were false-negative.

Possible explanations for discrepancies between somatostatin receptor imaging *in vivo* and somatostatin receptor status *in vitro* are multitudinous (21). A tumor may have several particularities that may lead to a false-negative SRS result. First, a low tumor cellularity combined with a low receptor density may not give sufficient specific binding to allow tumor detection *in vivo*. Because RT-PCR experi-

ments did not reveal any significant difference on mRNA level and immunocytochemical experiments showed a rather higher receptor density on the surface of ON meningioma cells and, furthermore, histology was not associated with a negative SRS result, this possibility can clearly be excluded. Second, tumors with a high endogenous somatostatin production may be found to be receptor negative *in vivo* because of occupancy of available somatostatin receptors. Numerous tumors are known to synthesize growth factors that stimulate their own growth in an autocrine or paracrine manner. In this way, most meningiomas are known to produce and secrete the platelet-derived growth factor and the epidermal growth factor (30). Also, somatostatin generally exhibiting antiproliferative effects (3,5) is known to stimulate growth of meningioma *in vitro* (6). However, to our knowledge, an endogenous somatostatin production of meningiomas has not been reported. Third, some somatostatin receptors may not be recognized because they belong to subtypes—for example, *sst1*—having no affinity to certain types of somatostatin analogs such as

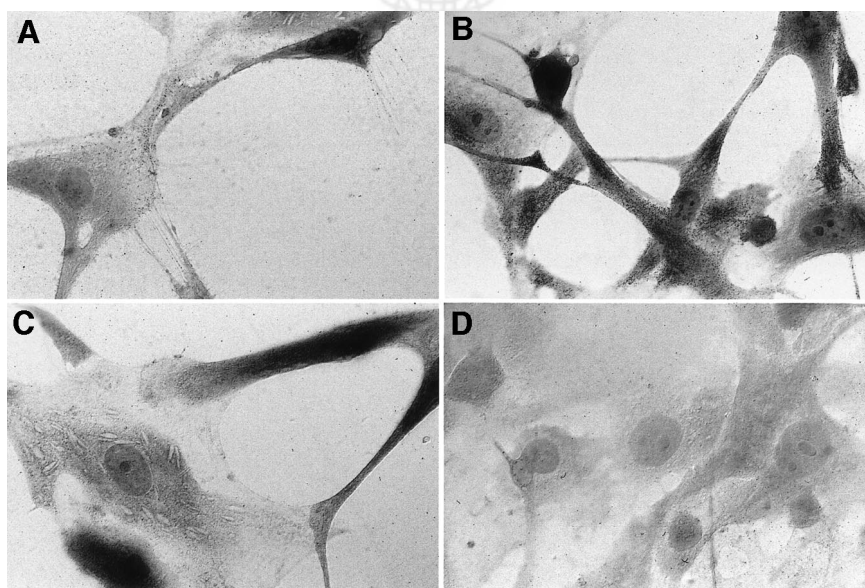


FIGURE 5. Immunocytochemical visualization of somatostatin receptor subtype 2 on surface of OP4 (A) and ON4 (B) cultivated cells. Control reactions were performed by preincubating primary antibody with surplus of its antigenic peptide, OP4 (C) or ON4 (D). (×170)

octreotide. For this reason, our *in vitro* studies were focused on *hsst2*. Fourth, a false-negative *in vivo* result may be obtained if the tumor is located in regions of high background activity such as the pituitary gland, the liver, the kidneys or the urinary bladder, in which *hsst2*-positive tumors may be masked. Because no association with these regions was found, this explanation does not account for the negative SRS result of meningiomas (12,20). Finally, SRS may fail to detect tumors that are located inside an intact permeability barrier (e.g., the blood–brain barrier). Because octreotide is a polar, water-soluble peptide, it cannot penetrate into those tumors that are provided with an intact permeability barrier (17–19). In particular, the sensitivity of about 100% of meningiomas in SRS was associated with the assumption that meningiomas are devoid of an intact blood–brain barrier (13–17).

Considering anatomic conditions, meningiomas are indeed devoid of a blood–brain barrier, but this does not necessarily allow the implication that meningiomas are accessible unrestrictedly for ^{111}In -octreotide in SRS. The system of the brain and its meninges, by far, is too complex for a model of 2 spaces (blood–brain) separated from each other by only 1 barrier to explain it. Moreover, several compartments exist that are flanked by different barriers (31). These compartments are again separated from the blood compartment by highly specific permeability barriers that are found mainly in 3 different locations (32). First, the endothelium of the cerebral vessels, including the closed envelope of astrocytic end feet, forms the blood–brain barrier in the strict sense (33). Second, the cerebrospinal fluid (CSF) of the brain ventricle, which is continuous with the cerebral interstitium, must be separated from the blood. Because of this requirement, 1 barrier is formed by the epithelium of the choroid plexus (34). Another site of leaky, fenestrated capillaries includes 6 of the 7 circumventricular organs where tanycytes hinder the free diffusion of plasma proteins from these blood vessels into the ventricle (35). Third, the outer CSF within the arachnoidal space, which is not strictly separated from the brain interstitium, must be separated from the hemal milieu of the dura. This task is performed by the CSF–blood barrier, which consists of the outer arachnoidal layer (31) that represents the outer layer of the outer leptomeningeal lamella (31). All of these barriers are characterized by 2 distinct properties: Tight junctions limit the paracellular flux and specific transport mechanisms control the transcellular flux. In a way that is similar to the manner in which the leptomeninges guarantees the function of the CSF–blood barrier, negatively charged extracellular glycoproteins and its 3 lamellae (inner, intermediate, and outer (31)) are responsible for delimitation of the other compartments (31,36). In addition, leptomeningeal tissue also provides an enzymatic barrier function, which protects the central nervous system from catecholamines produced in the periphery (35,37).

Bearing this in mind and taking under consideration that meningiomas are defined as tumors originating from cellu-

lar elements of the meninges, it is not surprising that meningioma cells in culture were found to reflect the barrier functions of the leptomeninges (38). Furthermore, whorl formation, or concentric wrapping of tumor cells around each another or around blood vessels in an onionskin pattern, is a well-known feature of meningiomas and probably represents a recapitulation of the function of leptomeningeal cells to cover surfaces and separate compartments (39). Accordingly, it is thinkable that meningiomas—especially in the beginning of their growth—meet the function of their tissue of origin to develop more-or-less intact permeability barriers that could give an explanation for the false-negative SRS result of meningiomas.

Therefore, permeability conditions of meningiomas were investigated in a further attempt using gadolinium-DTPA contrast-enhanced MRI and $^{99\text{m}}\text{Tc}$ -DTPA brain scintigraphy. Because gadolinium-DTPA and $^{99\text{m}}\text{Tc}$ -DTPA are extremely hydrophilic substances, they cannot cross the intact barriers of the central nervous system (18,19); thus, an accumulation is observed only under circumstances that lead to blood–brain barrier disruption (e.g., tumor, multiple sclerosis, and infection) (18,40). Whereas MRI always showed strong and homogeneous contrast enhancement and, thereby, suggested that meningiomas were devoid of a permeability barrier, all 5 ON meningiomas remained undetected by brain scintigraphy using $^{99\text{m}}\text{Tc}$ -DTPA (Table 1, group 3). Of 30 OP meningiomas investigated with both, SRS and brain scintigraphy using $^{99\text{m}}\text{Tc}$ -DTPA, 24 showed $^{99\text{m}}\text{Tc}$ -DTPA enhancement (Table 1, group 1), whereas 6 meningiomas remained undetected (Table 1, group 2). As expected from our previous results (12,20), the volume of ON meningiomas was much lower than the volume of $^{99\text{m}}\text{Tc}$ -DTPA–positive OP meningiomas. Additionally, it became evident that the volume of $^{99\text{m}}\text{Tc}$ -DTPA–negative OP meningiomas also was markedly lower than that of $^{99\text{m}}\text{Tc}$ -DTPA–positive OP meningiomas. Because the smallest $^{99\text{m}}\text{Tc}$ -DTPA–positive meningioma had a volume of 1.5 mL and the largest $^{99\text{m}}\text{Tc}$ -DTPA–negative meningioma had a volume of 19.3 mL an insufficient sensitivity can be excluded to account for negative $^{99\text{m}}\text{Tc}$ -DTPA results. Therefore, it can be concluded that brain scintigraphy had identified a permeability barrier, e.g., blood–tumor barrier as an explanation for the false-negative SRS results of ON meningiomas.

Because a small tumor size is associated with a false-negative SRS result, this blood–tumor barrier possibly more and more loses its integrity with progressive growth of the meningiomas. In the course of this increasing loss of barrier integrity, 1 method might still indicate an intact barrier function and another more sensitive method might imply free permeability conditions. As our results show, less intense uptake was noted in brain scintigraphy using $^{99\text{m}}\text{Tc}$ -DTPA than in SRS. This finding is in accordance with results published by 2 other groups (16,17), both of which speculated that the extravasation of the receptor-specific tracer ^{111}In -octreotide would result in stronger contrast than

the extravasation of nonspecific ^{99m}Tc -DTPA in *hsst2*-expressing tumors. Accordingly, SRS, because of its receptor specificity, most likely allows an earlier detection of a blood–tumor barrier disruption in *hsst2*-expressing meningiomas, which would fit to the observation that none of the meningiomas was positive for ^{99m}Tc -DTPA but was negative for ^{111}In -octreotide. Correspondingly, the blood–tumor barrier integrity of ON meningiomas was apparently insufficient to prevent contrast enhancement in MRI.

CONCLUSION

RT-PCR and immunocytochemistry showed that SRS-negative meningiomas do express *hsst2*. Thus, these negative SRS results are false-negative. Because an insufficient sensitivity was excluded, ^{99m}Tc -DTPA scintigraphy identified a permeability barrier in SRS-negative meningiomas that explains their false-negative SRS results. SRS-negative meningiomas—especially in the beginning of their growth—most likely meet the function of their tissue of origin (i.e., the meninges) to develop more-or-less intact permeability barriers. Because this is the first report of a blood–tumor barrier in meningiomas that might be of major importance for possible systemic therapy concepts in future, the nature of this barrier needs further investigation.

ACKNOWLEDGMENT

The development of the antibodies against the human somatostatin receptor subtype 2 protein was kindly supported by the German Research Foundation (grant DFG-Kr 569/7-1).

REFERENCES

- Epelbaum J. Somatostatin in the central nervous system: physiological and pathological modifications. *Prog Neurobiol*. 1986;27:63–100.
- Krulich L, Dhariwal AP, McCann SM. Stimulatory and inhibitory effects of purified hypothalamic extracts on growth hormone release from rat pituitary in vitro. *Endocrinology*. 1968;83:783–790.
- Liebow C, Reilly C, Serrano M, Schally AV. Somatostatin analogues inhibit growth of pancreatic cancer by stimulating tyrosine phosphatase. *Proc Natl Acad Sci USA*. 1989;86:2003–2007.
- Reubi JC, Krenning E, Lamberts SW, Kvolts L. In vitro detection of somatostatin receptors in human tumors. *Digestion*. 1993;54:76–83.
- Tahiri-Jouti N, Cambillau C, Viguier N, et al. Characterization of a membrane tyrosine phosphatase in AR42J cells: regulation by somatostatin. *Am J Physiol*. 1992;262:G1007–G1014.
- Koper JW, Markstein R, Kohler C, et al. Somatostatin inhibits the activity of adenylate cyclase in cultured human meningioma cells and stimulates their growth. *J Clin Endocrinol Metab*. 1992;74:543–547.
- Bakker WH, Krenning EP, Reubi JC, et al. In vivo application of [^{111}In -DTPA-D-Phe1]-octreotide for detection of somatostatin receptor-positive tumors in rats. *Life Sci*. 1991;49:1593–1601.
- Krenning EP, Kwekkeboom DJ, Oei HY, et al. Somatostatin receptor imaging of endocrine gastrointestinal tumors. *Schweiz Med Wochenschr*. 1992;122:634–637.
- Sarda L, Duet M, Zini JM, et al. Indium-111 pentetreotide scintigraphy in malignant lymphomas. *Eur J Nucl Med*. 1995;22:1105–1109.
- Bohuslavizki KH, Brenner W, Gunther M, et al. Somatostatin receptor scintigraphy in the staging of small cell lung cancer. *Nucl Med Commun*. 1996;17:191–196.
- Reisinger I, Bohuslavizki KH, Brenner W, et al. Somatostatin receptor scintigraphy in small-cell lung cancer: results of a multicenter trial. *J Nucl Med*. 1998;39:224–227.
- Bohuslavizki KH, Brenner W, Braunsdorf WE, et al. Somatostatin receptor scintigraphy in the differential diagnosis of meningioma. *Nucl Med Commun*. 1996;17:302–310.
- Hildebrandt G, Scheidhauer K, Luyken C, et al. High sensitivity of the in vivo detection of somatostatin receptors by ^{111}In (DTPA-octreotide)-scintigraphy in meningioma patients. *Acta Neurochir (Wien)*. 1994;126:63–71.
- Maini CL, Cioffi RP, Tofani A, et al. Indium-111 octreotide scintigraphy in neurofibromatosis. *Eur J Nucl Med*. 1995;22:201–206.
- Scheidhauer K, Hildebrandt G, Luyken C, Schomacker K, Klug N, Schicha H. Somatostatin receptor scintigraphy in brain tumors and pituitary tumors: first experiences. *Horm Metab Res Suppl*. 1993;27:59–62.
- Barth A, Haldemann AR, Reubi JC, et al. Noninvasive differentiation of meningiomas from other brain tumours using combined ^{111}In indium-octreotide/ ^{99m}Tc technetium-DTPA brain scintigraphy. *Acta Neurochir (Wien)*. 1996;138:1179–1185.
- Haldemann AR, Rosler H, Barth A, et al. Somatostatin receptor scintigraphy in central nervous system tumors: role of blood-brain barrier permeability. *J Nucl Med*. 1995;36:403–410.
- Rhine WD, Benaron DA, Enzmann DR, et al. Gd-DTPA MR detection of blood-brain barrier opening in rats after hyperosmotic shock. *J Comput Assist Tomogr*. 1993;17:563–566.
- Zelaya FO, Rose SE, Nixon PF, et al. MRI demonstration of impairment of the blood-CSF barrier by glucose administration to the thiamin-deficient rat brain. *Magn Reson Imaging*. 1995;13:555–561.
- Klutmann S, Bohuslavizki KH, Tietje N, et al. Clinical value of 24-hour delayed imaging in somatostatin receptor scintigraphy for meningioma. *J Nucl Med*. 1999;40:1246–1251.
- Reubi JC. Neuropeptide receptors in health and disease: the molecular basis for in vivo imaging. *J Nucl Med*. 1995;36:1825–1835.
- Mentlein R, Buchholz C, Krisch B. Somatostatin-binding sites on rat telencephalic astrocytes: light- and electron-microscopic studies in vitro and in vivo. *Cell Tissue Res*. 1990;262:431–443.
- Parwaresch MR, Radzun HJ, Kreipe H, Hansmann ML, Barth J. Monocyte/macrophage-reactive monoclonal antibody Ki-M6 recognizes an intracytoplasmic antigen. *Am J Pathol*. 1986;125:141–151.
- Dournaud P, Gu YZ, Schonbrunn A, Mazella J, Tannenbaum GS, Beaudet A. Localization of the somatostatin receptor SST2A in rat brain using a specific anti-peptide antibody. *J Neurosci*. 1996;16:4468–4478.
- McConachie NS, Worthington BS, Cornford EJ, Balsitis M, Kerslake RW, Jaspas T. Computed tomography and magnetic resonance in the diagnosis of intraventricular cerebral masses. *Br J Radiol*. 1994;67:223–243.
- Patel YC, Srikant CB. Subtype selectivity of peptide analogs for all five cloned human somatostatin receptors (hsstr 1–5). *Endocrinology*. 1994;135:2814–2817.
- John M, Meyerhof W, Richter D, et al. Positive somatostatin receptor scintigraphy correlates with the presence of somatostatin receptor subtype 2. *Gut*. 1996;38:33–39.
- Perez J, Rigo M, Kaupmann K, et al. Localization of somatostatin (SRIF) SSTR-1, SSTR-2 and SSTR-3 receptor mRNA in rat brain by in situ hybridization. *Naunyn Schmiedebergers Arch Pharmacol*. 1994;349:145–160.
- Reisine T, Bell GI. Molecular biology of somatostatin receptors. *Endocr Rev*. 1995;16:427–442.
- McCutcheon IE. The biology of meningiomas. *J Neurooncol*. 1996;29:207–216.
- Krisch B, Leonhardt H, Oksche A. The meningeal compartments of the median eminence and the cortex: a comparative analysis in the rat. *Cell Tissue Res*. 1983;228:597–640.
- Rascher G, Wolburg H. The tight junctions of the leptomeningeal blood-cerebrospinal fluid barrier during development. *J Hirnforsch*. 1997;38:525–540.
- Dermietzel R. Junctions in the central nervous system of the cat. 3. Gap junctions and membrane-associated orthogonal particle complexes (MOPC) in astrocytic membranes. *Cell Tissue Res*. 1974;149:121–135.
- van Deurs B, Koehler JK. Tight junctions in the choroid plexus epithelium: a freeze-fracture study including complementary replicas. *J Cell Biol*. 1979;80:662–673.
- Gherzi-Egea JF, Leininger-Muller B, Cecchelli R, Fenstermacher JD. Blood-brain interfaces: relevance to cerebral drug metabolism. *Toxicol Lett*. 1995;82–83:645–653.
- Krisch B, Leonhardt H, Oksche A. Compartments and perivascular arrangement of the meninges covering the cerebral cortex of the rat. *Cell Tissue Res*. 1984;238:459–474.
- Edvinsson L. Innervation of the cerebral circulation. *Ann N Y Acad Sci*. 1987;519:334–348.
- Feurer DJ, Weller RO. Barrier functions of the leptomeninges: a study of normal meninges and meningiomas in tissue culture. *Neuropathol Appl Neurobiol*. 1991;17:391–405.
- Manivel JC, Sung JH. Pathology of meningiomas. *Pathol Annu*. 1990;25:159–192.
- Spigelman MK, Zappulla RA, Johnson J, Goldsmith SJ, Malis LI, Holland JF. Etoposide-induced blood-brain barrier disruption: effect of drug compared with that of solvents. *J Neurosurg*. 1984;61:674–678.